Virus Research 263 (2019) 102–111

Contents lists available at ScienceDirect

Virus Research

journal homepage: www.elsevier.com/locate/virusres

Cetylpyridinium chloride interaction with the hepatitis B virus core protein inhibits capsid assembly

Hyun Wook Seo[a], Joon Pyung Seo[a], Yuri Cho[b], Eunkyong Ko[a], Yoon Jun Kim[c], Guhung Jung[a,*]

[a] Department of Biological Sciences, College of Natural Sciences, Seoul National University, 599 Gwanak-ro, Gwanak-gu, Seoul, 151-747, South Korea
[b] Department of Internal Medicine, CHA Gangnam Medical Center, CHA University School of Medicine, Seoul, 06125, South Korea
[c] Department of Internal Medicine and Liver Research Institute, Seoul National University College of Medicine, Seoul, 03080, South Korea

ARTICLE INFO

Keywords:
Antiviral
Capsid assembly inhibitor
Drug synergism
Cetylpyridinium chloride (CPC)
Hepatitis B virus (HBV)

ABSTRACT

Hepatitis B virus (HBV) infection is a major risk factor for chronic liver disease, cirrhosis, and hepatocellular carcinoma (HCC) worldwide. While multiple hepatitis B drugs have been developed, build up of drug resistance during treatment or weak efficacies observed in some cases have limited their application. Therefore, there is an urgent need to develop substitutional pharmacological agents for HBV-infected individuals. Here, we identified cetylpyridinium chloride (CPC) as a novel inhibitor of HBV. Using computational docking of CPC to core protein, microscale thermophoresis analysis of CPC binding to viral nucleocapsids, and *in vitro* nucleocapsid formation assays, we found that CPC interacts with dimeric viral nucleocapsid protein (known as core protein or HBcAg) specifically. Compared with other HBV inhibitors, such as benzenesulfonamide (BS) and sulfanilamide (SA), CPC achieved significantly better reduction of HBV particle number in HepG2.2.15 cell line, a derivative of human HCC cells that stably expresses HBV. CPC also inhibited HBV replication in mouse hydrodynamic model system. Taken together, our results show that CPC inhibits capsid assembly and leads to reduced HBV biogenesis. Thus, CPC is an effective pharmacological agent that can reduce HBV particles.

1. Introduction

Hepatitis B virus (HBV) causes chronic hepatitis, and the number of infections is rapidly increasing each year (Ott et al., 2012; Zuckerman, 1999). Chronic HBV infection is closely associated with the development of cirrhosis and hepatocellular carcinoma (HCC) (Paradis, 2013). The partially double-stranded DNA genome of HBV is 3.2 kb in size, and encodes 4 distinct proteins: core protein, surface protein (large, middle, small), X protein, and a polymerase capable of both DNA-dependent and RNA-dependent DNA polymerization (Seeger and Mason, 2000). During the course of infection, the HBV genome is transformed into covalently closed circular DNA (cccDNA) with the aid of the nucleus repair system (Seeger and Mason, 2000). The cccDNA then serves as a template for transcription of pregenomic RNA (pgRNA) by the host's RNA polymerase (Seeger and Mason, 2000). HBcAg can be assembled into T = 3 or T = 4 icosahedral capsid structures, and an envelope is formed from insertion of surface antigens into the host intracellular membrane (Seeger and Mason, 2000).

HBV has been researched by biologists and pharmacologists, and multiple therapeutics have been developed to inhibit viral replication (Stein and Loomba, 2009). For example, lamivudine (LAM) and adefovir were introduced as HBV replication inhibitors, and were administered to treat HBV infections. These nucleos(t)ide analogue drugs usually induce drug resistance and show low efficacy (Doong et al., 1991). While the recently developed entecavir, telbivudine and tenofovir demonstrated less drug resistance, insufficient studies on these drugs were conducted; results indicated that they vary in efficiency between patients, and induce other mutant resistance as a side effect (Pan et al., 2017). Thus, previous treatment regimens for these HBV replicative inhibitor drugs involved diverse combinatorial administration depending on an individual's susceptibility to each drug species (Brunetto and Lok, 2010). Therefore, there is increased attention and demand for new drugs that target different parts of the HBV infection process. One potential mechanism of action is to inhibit capsid

Abbreviations: HBV, hepatitis B virus; HBcAg, hepatitis B core antigen; DMSO, dimethyl sulfoxide; BS, benzenesulfonamide; IDO, idoxuridine; CPC, cetylpyridinium chloride; AMO, amoxicillin; TPH, tripelennamine HCl; FLU, fluocinonide; GLI, gliquidone; RFC, rofecoxib; AML, amlodipine besylate; CLZ, clozapine; TET, tetracycline HCl SA sulfanilamide; LAM, lamivudine

* Corresponding author at: Department of Biological Sciences, College of Natural Sciences, Seoul National University, 599 Gwanak-ro, Gwanak-gu, Seoul, 151-747, South Korea.
E-mail address: drjung@snu.ac.kr (G. Jung).

https://doi.org/10.1016/j.virusres.2019.01.004
Received 27 November 2018; Received in revised form 8 January 2019; Accepted 9 January 2019
Available online 09 January 2019
0168-1702/

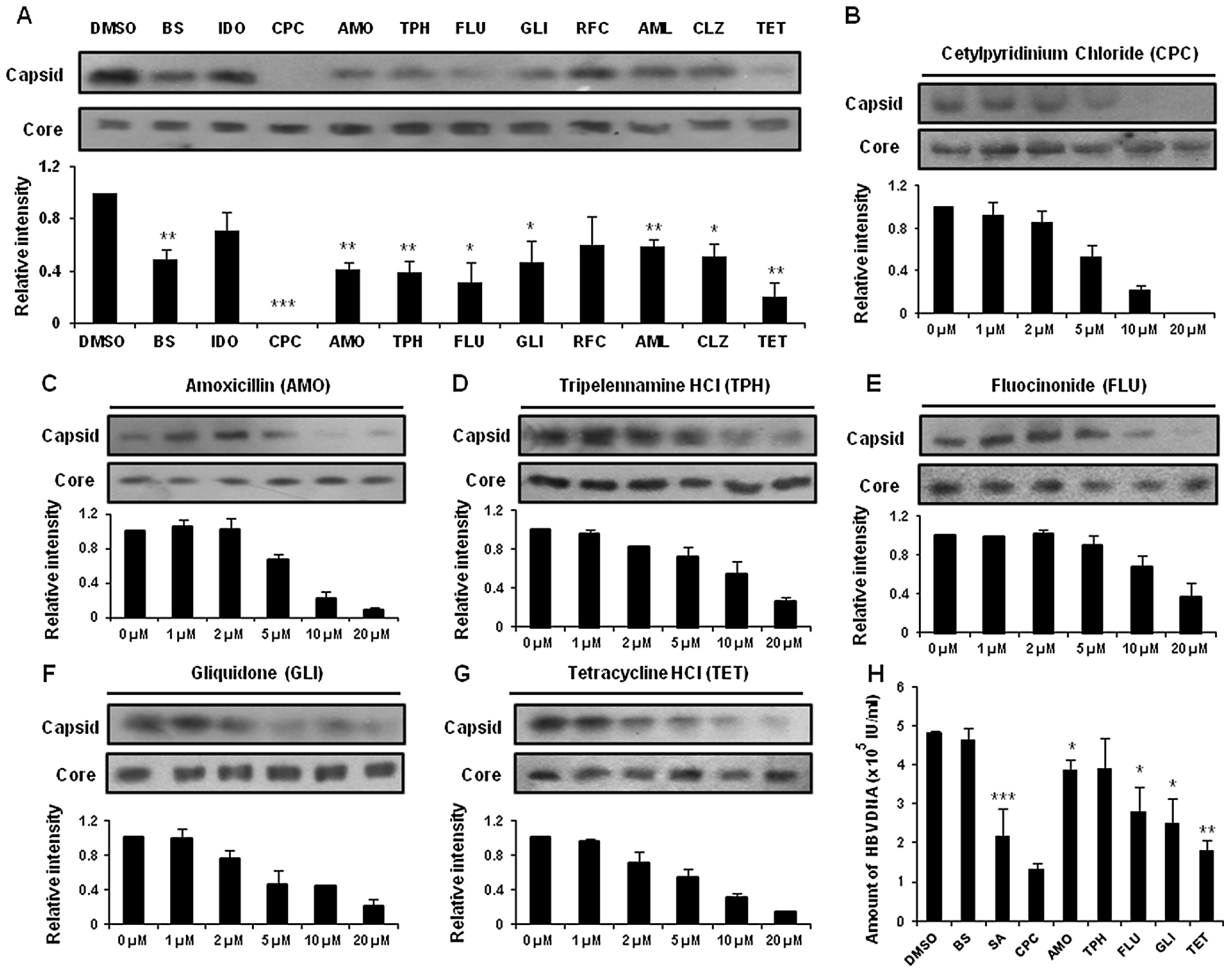

Fig. 1. CPC inhibits HBV capsid assembly *in vitro*.
A. Capsid assembly assay with HBV Cp149 and candidates (20 μM) for inhibiting HBV capsid assembly.
B-G. Capsid assembly assay using HBV capsid inhibitor candidates (0–20 μM). IC_{50} of CPC was measured as an average of the immunoblot band intensity.
H. Quantitation of HBV DNA following treatment with 1 μM core assembly inhibitors.
Values are mean ± standard error of the mean (SEM, n = 4 per group); $*p < 0.05$, $**p < 0.01$, and $***p < 0.001$, *t* test.
HBV, Hepatitis B virus; Cp149, Core protein 149; DMSO, Dimethyl sulfoxide; BS, Benzenesulfonamide; IDO, Idoxuridine; CPC, Cetylpyridinium chloride; AMO, Amoxicillin; TPH, Tripelennamine HCl; FLU, Fluocinonide; GLI, Gliquidone; RFC, Rofecoxib; AML, Amlodipine besylate; CLZ, Clozapine; TET, Tetracycline HCl, SA, Sulfanilamide.

assembly, which in turn inhibits replication and build up of virus particles (Vanlandschoot et al., 2003).

Our research focused on targeting the HBV capsid; the core protein has 183–185 amino acids with two functional domains (Hirsch et al., 1990). Assembly domain (1–149 aa) interacts with neighboring core proteins to form the icosahedral capsid structure, while protamine domain (150–183/185 aa) interacts with pgRNA to regulate reverse transcriptase (RTs) activity (Hirsch et al., 1990; Wynne et al., 1999). To determine its exact effect on *in vitro* capsid assembly, we used a C-terminal region truncated, assembly domain of the core protein; Cp149. Cp149 form dimers and three dimers assemble into a hexamer structure. The Cp149 hexamer acts as a nucleus and stabilizes capsid assembly (Lott et al., 2000).

In a previous study, cetylpyridinium chloride (CPC) was shown to possess anti-bacterial activity (Popkin et al., 2017). Nevertheless, the inhibitory effect of CPC against Hepatitis B virus remains to be elucidated. Capsid inhibitors such as benzenesulfonamide (BS) and sulfanilamide (SA) inhibit HBV capsid assembly at relatively high half maximal inhibitory concentrations (IC_{50}; 7–200 μM) (Cho et al., 2014, 2013). In this paper, we found that CPC interfered with HBV capsid assembly with a low IC_{50} (2–3 μM). We aimed to determine the functional role of CPC in HBV capsid assembly and demonstrated that CPC significantly decreased HBV biogenesis through binding to dimeric core proteins, in consequence, preventing capsid formation.

2. Materials and Methods

2.1. Purification of Cp149, HBV capsid assembly analysis, and sucrose density gradient analysis

Cp149 gene from pHBV1.2x template was amplified using a forward primer, 5′-ACCATGGACATTGACCCGTATAAAG-3′, including an NcoI site and a reverse primer, 5′-ACTCGAGTTAAACAACAGTAGTTTC CGG-3′ including an XhoI site. Amplified Cp149 gene was then ligated into pGEMT-easy vector (Promega, Madison, USA) and transformed into DH5α cell. Then the amplified Cp149 gene was restricted at the NcoI and XhoI enzyme site and ligated into pET28b E. coli expression vector (Novagen, Madison, WI). The pET28b/Cp149 plasmid was transformed into BL21(DE3) + pLysS *Escherichia coli* expression host (Novagen, Madison, USA) (Choi et al., 2005). Cp149 was induced by 1 mM isopropyl-ß-D-thiogalactopyranoside (IPTG) and incubated at 37°C for 4 h. Cp149 dimers were stored in stock solution (100 mM glycine (pH 9.5), 10% glycerol) at -70°C. Capsid assembly reaction was conducted in assembly reaction buffer (50 mM HEPES, 15 mM NaCl,

Table 1
ADMET property of HBV inhibitor candidates. ADMET analysis was conducted based on six distinct criteria. Solubility in log S value was predicted as an important determinant in absorption. Plasma protein binding (PPB) affinity level and blood brain barrier (BBB) penetration confidence status were introduced as distribution criteria. Cytochrome P450 2D6 (CYP2D6), an enzyme deeply involved in xenobiotic metabolism, was ssubjected to inhibition probability computation for drug metabolism and excretion evaluation. Hepatotoxicity probability was predicted among other toxicities. Molecular partition coefficient (AlogP98) and polar surface area (PSA2D) values were plotted showing absorption and blood.

		ADMET									
Name	FDA approved drug number (Selleckchem, Cat. L1300)	Solubility	PPB level	Hepatotoxicity probability	CYP2D6 probability	AlogP98	PSA 2D	Absorption-95	Absorption-99	BBB-95	BBB-99
Sulfanilamide (SA)		−0.891	0	0.649	0.039	−0.212	87.681	✓	✓	✓	✓
Benzenesulfonamide (BS)		−1.365	0	0.536	0.049	0.535	61.141	✓	✓		✓
Idoxuridine (IDO)	357	−0.213	0	0.761	0.099	−1.208	101.325		✓		
Cetylpyridinium chloride (CPC)	849	−6.305	2	0.589	0.722	7.584	5.348				
Amoxicillin (AMO)	649	−2.523	0	0.364	0.445	−0.06	136.236		✓		
Tripelennamine HCl (TPH)	704	−3.702	1	0.635	0.881	3.102	17.965	✓	✓	✓	✓
Fluocinonide (FLU)	632	−3.88	0	0.344	0.326	1.374	99.508	✓	✓		✓
Gliquidone (GLI)	708	−5.735	2	0.344	0.297	4.738	124.406				
Rofecoxib (RFC)	666	−4.258	1	0.701	0.514	2.871	60.832	✓	✓	✓	✓
Amlodipine besylate (AML)	326	−3.593	2	0.284	0.495	1.576	100.742	✓	✓		✓
Clozapine (CLZ)	534	−5.176	2	0.238	0.732	3.476	30.838	✓	✓	✓	✓
Tetracycline HCl (TET)	610	−2.648	0	0.854	0.326	−1.011	185.872				
Entecavir		−0.528	0	0.39	0.396	−1.404	126.214		✓		
Tenofovir		−1.086	0	0.748	0.148	−0.911	133.533		✓		
Adefovir		−3.546	0	0.331	0.326	1.899	162.224				
Lamivudine		−0.83	0	0.364	0.059	−0.59	88.262	✓	✓		✓
Telbivudine		−0.102	0	0.801	0.039	−1.044	101.325	✓	✓		

Solubility : log S, 10-based logarithm of the aqueous solubility in mol/L.
CYP2D6 : Cytochrome P450 2D6 enzyme inhibition probability.
PPB : level of Plasma Protein Binding affinity.
AlogP98 : the logarithm of the partition coefficient between n-octanol and water.
PSA 2D : polar surface area.
Absorption/ BBB : confidence in Human Intestine Absorption and Blood Brain Barrier penetration.

10 mM $CaCl_2$ (pH 7.5)) with candidate drug concentration (ranging from 1 to 20 μM) at 37 °C for 1 h. Assembled particles were detected by immunoblot analysis using mouse monoclonal anti-HBV core antibody (Abcam, Cambridge, UK). The core dimer protein, given in equivalent quantity in every test samples, were acquired in same volume before processing the capsid assembly reaction for immunoblot analysis and were given as input normalization control (Kim et al., 2015). Sucrose density gradient analysis was conducted by ultracentrifugation (HITACHI, Tokyo, Japan) for 3.5 h at 250,000 *g*. Samples were prepared after SA (200 μM), BS (200 μM) and CPC (20 μM) treatments. Fractions of sucrose concentrations were analyzed by 15% SDS-PAGE followed by immunoblot analysis using mouse monoclonal anti-HBV core antibody (Abcam, Cambridge, UK) (Kang et al., 2006).

2.2. Measurement of cell viability

Cell viability was determined by the 3-(4,5-dimethylthiazol-2-yl)-2,5-diphenyltetrazolium bromide (MTT) assay. HepG2.2.15 cells were cultured at 80% confluency in 96-well plates and maintained in Dulbecco's modified Eagle's medium (DMEM, Wellgene, Gyeongsan-si, South Korea). The cells were treated with varying concentrations 0 to 1 μM of CPC for 24 h and then washed with PBS and treated with the MTT solution for 4 h at 37℃. Absorbance at 570 nm was measured using a microphotometer reader (BioTek, Vermont, USA) (Lee et al., 2013). Examination on HepG2.2.15 cells were practiced within drug concentration range from 0 to 1 μM while drug concentrations greater than 1 μM were tested only for *in vitro* capsid assembly experiments.

2.3. CPC in silico docking modeling

We built in silico Cp149 dimer structure from X-ray crystallography data (PDB ID: 1QGT) using Discovery studio 2.5 (Accelrys, San Diego, USA). Simulations were based on the CHARMM force field, and Momany-Rone partial charge method (Wu et al., 2003). We used LibDock (Rao et al., 2007), LigandFit (Venkatachalam et al., 2003), and CDOCKER (Wu et al., 2003) algorithms to screen candidate molecules that fit into cavity structures of the Cp149 dimer. Optimal binding poses with highest receptor-ligand scores were searched. Energy level was minimized through the Adopted Basis-set Newton-Raphson algorithm, and the obtained structures were equilibrated at 37℃ for 100,000 cycles (Leis et al., 2010; Smith et al., 2012).

2.4. Protein–small molecule interaction analysis using microscale thermophoresis

Cp149 and other proteins (BSA, anti-TAK1, anti-GST, anti-MDM2, Pac1) were labeled with Monolith NT.115 protein labeling kit RED (Nanotemper, Munich, Germany), and was eluted to 10 μg in the MST buffer (50 mM Tris−HCl (pH 7.4), 150 mM NaCl, 10 mM MgCl2, and 0.05% Tween-20). CPC was serially diluted (0.02–100 μM) into Cp149 solutions. Samples were incubated at 37℃ for 10 min, and were analyzed using the Monolith NT.115 program (Nanotemper, Munich, Germany). All the experiments were performed thrice and analyzed as previously described (Timofeeva et al., 2012).

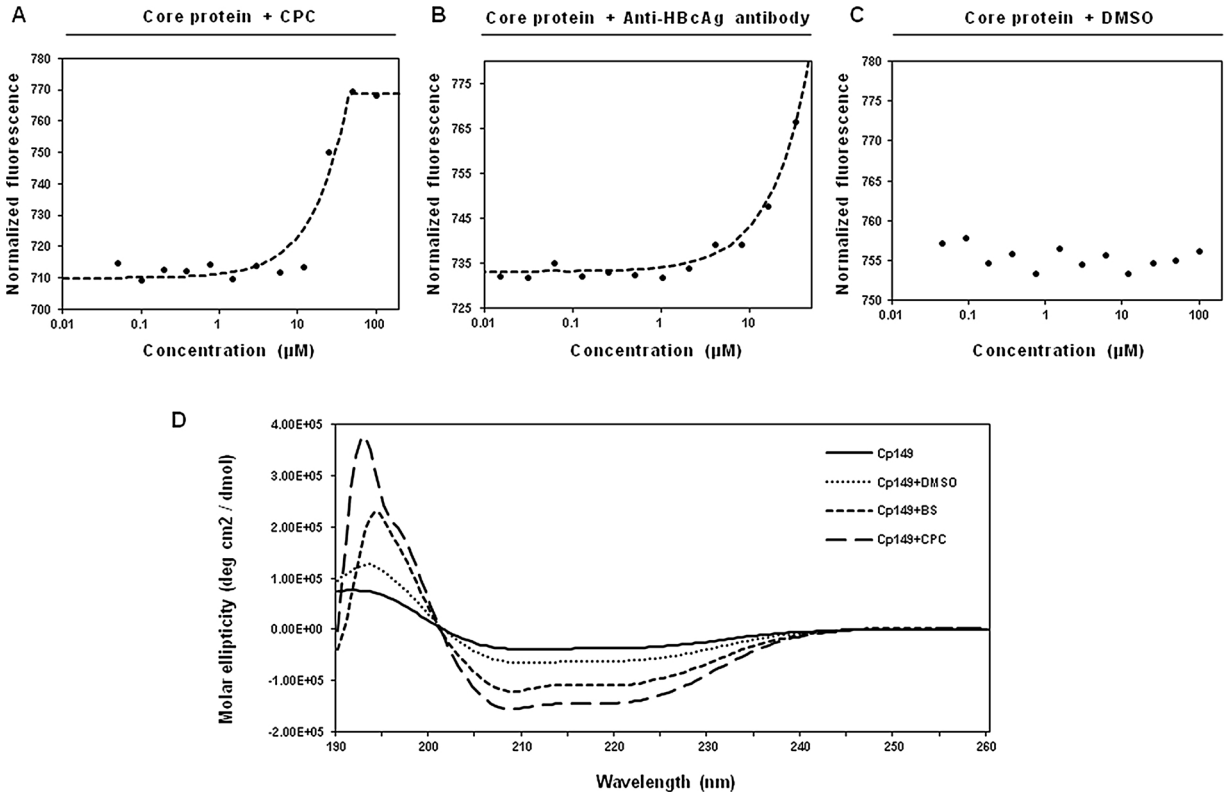

Fig. 2. Interaction and conformational change of HBV Cp149 with the novel capsid assembly inhibitor CPC.
A-C. Microscale thermophoresis changes between purified Cp149 and CPC (A), Anti-HBcAg antibody (B, Positive control), and DMSO (C, Negative control). Experiments were repeated in 20, 40, 60, and 80% MST power sequences and results from 40% MST are presented in the figure.
D. Molar ellipticity change in Cp149 with 1% DMSO (Negative control), 50 μM BS (Positive control), and 5 μM CPC treatment.
HBV, Hepatitis B virus; Cp149, Core protein 149; DMSO, Dimethyl sulfoxide; Anti-HBcAg, Anti-Hepatitis B core antigen; BS, Benzenesulfonamide; CPC, Cetylpyridinium chloride.

2.5. Quantification of intracellular and extracellular HBV DNA, RNA by real-time PCR

HepG2.2.15 cells were treated with 978 FDA-approved chemicals (1 μM) (Cat. L1300, 978 drug compounds library version, Selleckchem, Houston, USA). Following 24 h incubation, media from each sample were collected and the extracellular HBV DNA was extracted using the phenol-chloroform extraction method. Cells were isolated from the media separately, sonicated for cell lysis, and centrifuged at 4°C, 12,000 rpm for 15 min. Intracellular HBV DNA was extracted from the supernatant using the phenol-chloroform extraction method. RNA was isolated from cells by using RNA Ribozol extraction reagent (Amresco, Ohio, USA) and reverse transcription was performed by using RT-DryMIX reverse transciptase (Enzynomics, Daejeon, South Korea). Total viral DNA and cDNA were measured by quantitative PCR using SYBR-Green mixture (Enzynomics, Daejeon, South Korea). The forward primer sequence was 5′-TCCTCTTCATCCTGCTGCTATG-3′, and reverse primer sequence was 5′-CGTGCTGGTAGTTGATGTTCCT-3′ (Garson et al., 2005; Shim et al., 2011).

2.6. CPC and LAM combination analysis using compusyn

To evaluate CPC and LAM synergism, we treated HepG2.2.15 cells grown in 96-well plates with CPC and LAM in various concentrations (0.01–1 μM) and ratios (12:1 to 0.33:1). After 24 h, the medium was collected and extracellular HBV DNA was extracted from the medium using the phenol-chloroform extraction method. The concentration of the extracellular HBV DNA was measured using quantitative PCR. IC_{50} and combination-index (CI) values were calculated using Compusyn (Molecular Pharmacology and Chemistry program, New York, USA). Single drug treatments and combination drug treatment dose-effect curves were fitted into logarithmic functions converging toward the discrete upper bounds in fractional effect value. IC_{50} values were obtained from the dose-effect curves. Dose reduction index (DRI) was calculated as the ratio of input dose in combinatorial treatment and corresponding single treatment dose in account with equal effect value. CI was calculated by adding the reciprocal value of each DRI for indicating synergism (CI $>$ 1, antagonistic effect; CI = 1, additive effect; CI $<$ 1, synergistic effect) (Chou, 2006, 2010).

2.7. Numerical analysis of capsid assembly inhibition

Based on the molecular simulation, searching for the difference in solvent accessibility between the protomer and free dimeric core protein, we identified the binding sites of contiguous protomers and CPC on the dimeric core protein, $Cp149_2$. Assembly inhibition was summarized into a competing equilibrium between CPC binding and capsid assembly (Table 4 Eq. 1, 2). Calculations of association constants K_{capsid} and K_{CPC} were based on the equilibria and mass-conservation law (Table 4 Eq. 3, 4). The equilibrium between $Cp149_2$ and capsid is represented by, K_{capsid} (Table 4 Eq. 5). Equations were recast in terms of capsid and CPC bound $Cp149_2$ concentrations (Table 4 Eq. 6, 7). The approach in calculating K_{capsid} using a 120th power multivariate function would yield consistent results for free dimer concentration in approximation. Consequently, capsid and CPC bound dimer concentrations is expressed to be linearly and inversely proportional to each other. $[Cp149_2]_{Total}$ and $[CPC]_{Total}$ are already known and values for $[Capsid]$ and K_{capsid} were determined experimentally (Zlotnick et al., 2002). Capsid assembly detected by immunoblot was interpreted, postulating the absence of protomer oligomers other than the capsid.

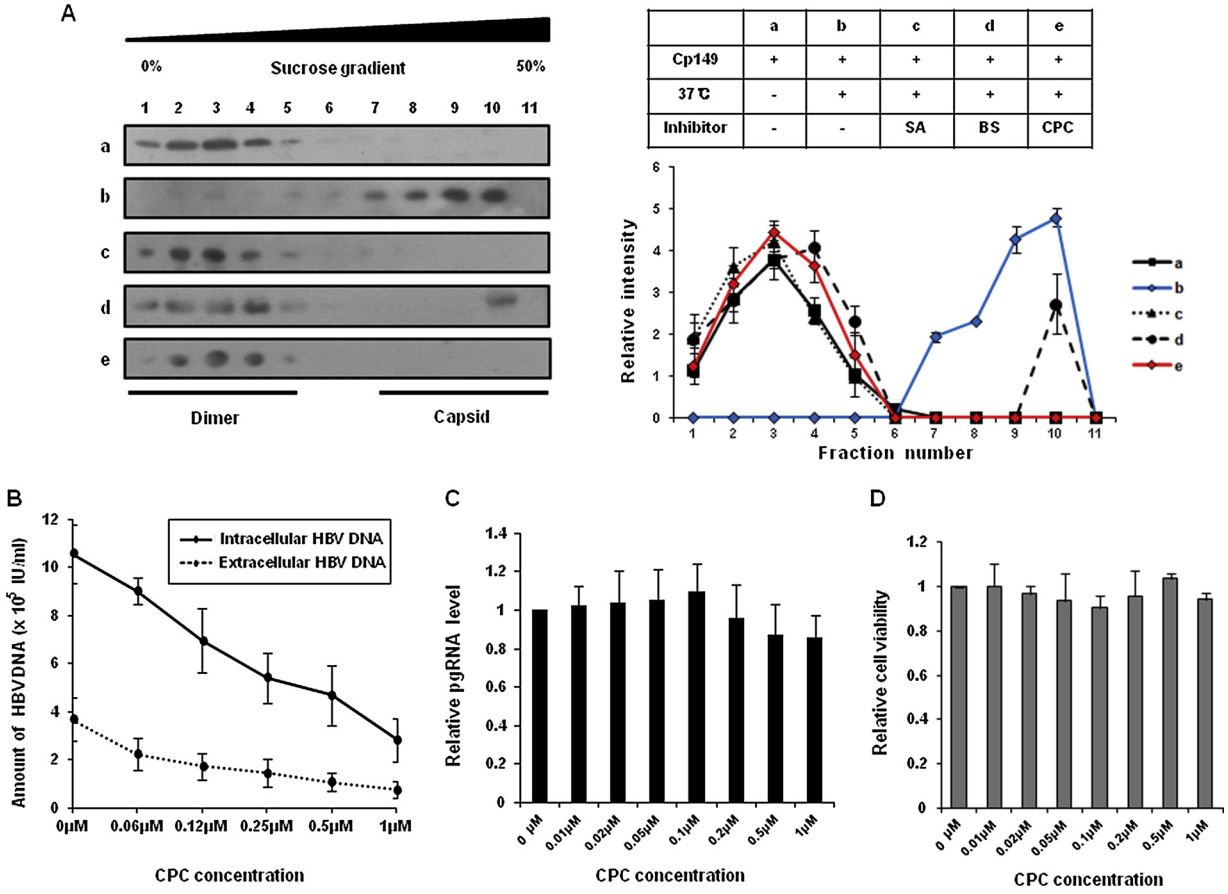

Fig. 3. Inhibition of HBV capsid assembly by CPC *in vivo*.
A. Sucrose density analysis of capsid assembly with DMSO, 200 μM SA, 200 μM BS, or 20 μM CPC. Non-assembled core protein (a), Fully-assembled core protein (b), Full-assembled core protein with 200 μM SA (c), 200 μM BS (d), 20 μM CPC (e) treatment.
B. Quantitation of HBV DNA following treatment with CPC (0–1 μM) in HepG2.2.15 cells.
C. Relative DNA quantity at the viral RNA transcription step of the HBV life cycle from HepG2.2.15 in a series of varying CPC concentration treatment.
D. HepG2.2.15 cell viability at series of CPC concentrations.
HBV, Hepatitis B virus; CPC, Cetylpyridinium chloride; DMSO, Dimethyl sulfoxide; SA, Sulfanilamide; BS, Benzenesulfonamide.

The CPC association constant was calculated and the inhibition curve was plotted with extrapolated prediction curve. Microscale thermophoresis was interpreted based on the superpositional expression of normalized fluorescence (Table 4 Eq. 8). The Soret coefficient was approximated for capsid particle in terms of $Cp149_2$ soret coefficient, based on geometrical symmetry and solvent accessibility calculation. Capsid structure was modeled into a spherical symmetric geometry for area calculation and virtual mole fraction coefficient of the capsid. Optimal Soret coefficients and assembly inhibitor association constants were found using the bisection method up to two significant digits. A thermophoretic curve was computed and CPC association constant was obtained (Baaske et al., 2010).

2.8. Circular dichroism (CD) analysis

CD analysis was carried out with J-815 (Jasco, Oklahoma City, USA). Spectra were measured using 1 nm bandwidth, scan speed 50 nm/min, response time of 1 s and three accumulations. The CD measurements were made using a quartz cuvette with a 1 cm path length and total protein concentration of 0.1 mg/mL. Values were measured by Spectra manager and Spectra analysis version 2.01 A program (Zlotnick et al., 2002).

2.9. Transmission electron microscopy (TEM)

For negative staining, 10 μL of assembled Cp149 samples were applied to each carbon-coated grid, and were incubated for 1 min; the grid was stained with 2% uranyl acetate. TEM was conducted on a LIBRA 120 (Carl Zeiss, Oberkochen, Germany) operating at 120 KV at the NICEM (National Instrumentation Center for Environmental Management, Seoul, South Korea). Three conditions including condition without capsid assembly, condition with capsid assembly, and condition with capsid assembly under 20 μM CPC treatment were imaged with electron microscopy. Numbers of capsid particles in equivalent size of area were counted. Capsid particles were classified into three categories: normal, broken, or aberrant capsid. Broken capsid was defined as a spherical, capsid-like structure that is partially broken. Aberrant capsid was defined as a particle that has detectable size (Kang et al., 2006).

2.10. Mouse model system

The HBV genome (from Wang-Shick Ryu, Addgene plasmid (#51294; Addgene, Watertown, USA)) was cloned into the pAAV vector to generate the HBV replicative plasmid pAAV-HBV1.2 × . Six-week-old male C57BL/6 mice were injected with the plasmid *via* the tail vein (n = 5/group) and then injected intramuscularly with CPC (272 μg/kg/day) daily. Serum samples were collected daily from the orbital sinus of the mice to measure HBV DNA by real-time PCR. The animals were sacrificed by CO_2 gassing 4 days after injection of pAAV-HBV1.2 × . All animal studies were conducted in accordance with ethical regulations under protocols approved by the Institutional Animal Care and Use

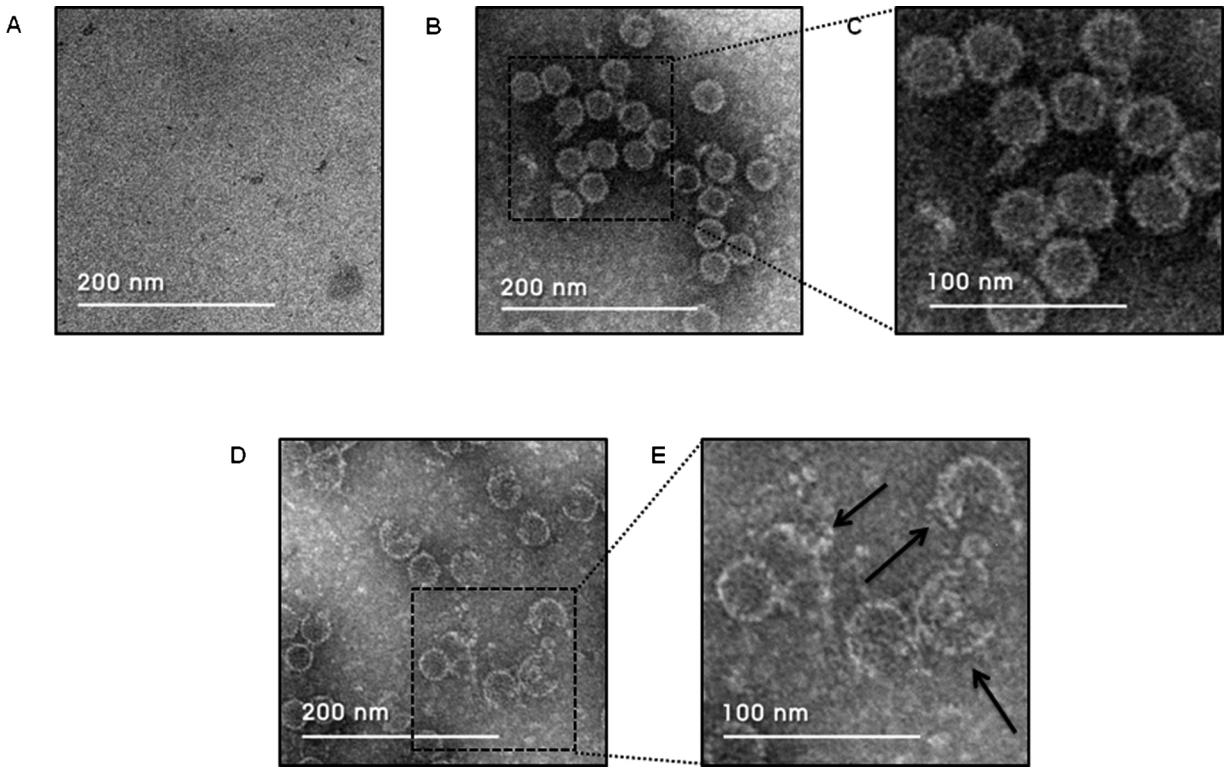

Fig. 4. Transmission electron micrographs of untreated and CPC-treated Cp149 capsids.
A. Non-assembled Cp149.
B. Fully assembled Cp149 in reaction buffer at 37 °C with no treatment.
C. Magnified image of fully assembled capsid particle with no treatment.
D. Assembled Cp149 with 20 μM CPC treatment.
E. Magnified image of broken capsid particles after 20 μM CPC treatment.
Cp149, Core protein 149; CPC, Cetylpyridinium chloride.

Table 2
Capsid particle classification. Capsid particles in each case, pre-reaction, post-reaction, and post-reaction with 20 μM CPC treatment, were counted and classified into one of the following categories: normal capsid, broken capsid, and abnormal capsid. Broken capsid was defined as those that resemble normal capsids, but with significantly disrupted spherical structures. Abnormal capsids have significant size but, resemble neither normal capsid nor broken capsid. Most particles classified as abnormal capsids were amorphous aggregates with similar sizes as capsids.

	Capsid counts			
Number	Normal	Broken	Abnormal forms	Total counts
Non-assembled	40	2 (4.65%)	1 (2.32%)	43
Fully assembled	944	49 (4.78%)	31 (3.02%)	1024
Cetylpyridinium chloride	83	203 (51.26%)	110 (27.77%)	396

Committee of CHA University (IACUC-170049).

3. Results

3.1. Capsid assembly assay revealed that CPC is a potent drug for abolishing HBV

HepG2.2.15 cells were treated with FDA-approved chemicals (Cat. L1300, 978 drug compounds library version, Selleckchem, Houston, USA). Out of the 978 chemicals approved by the FDA, 100 chemicals that induced the greatest reduction in viral particles, as assessed by real-time PCR, were selected as first candidates. First candidates were tested for HBV capsid assembly inhibition, and top 10 candidates were selected for further analysis (Fig. 1A, Table 1). The HBV core protein Cp149 was treated with 6 out of the 10 chemicals, including CPC (0–20 μM) (Fig. 1B–G). Among the 6 candidates, CPC showed the most effective capsid assembly inhibition with an IC_{50} of 2.5 ± 0.5 μM while other candidates (AMO, TPH, FLU, GLI, TET) showed IC_{50} greater than 5 μM (Fig. 1B–G). CPC was more effective in inhibiting HBV viral replication than other drug candidates (Fig. 1H). These data suggested that CPC is effective in blocking HBV capsid assembly.

3.2. CPC interacted and induced conformational change in the HBV Cp149 dimer

The monolith assay is based on thermodynamic changes that denote interactions between proteins and small molecules (Timofeeva et al., 2012). Results indicated that CPC interacts with the HBV Cp149 dimer (Fig. 2A). Anti-HBcAg antibodies (Smith et al., 2012) and DMSO were used as positive and negative controls, respectively (Fig. 2B, 2C). CPC showed interaction propensity, unlike DMSO (Fig. 2). Automatically calculated dissociation constants for 1:1 stoichiometric 1st order reactions were 9.9776 μM and 2.2998 μM for CPC and anti-HBcAg antibody, respectively. Dissociation constant for DMSO was undefined, indicating that DMSO doesn't interact with the Cp149 dimer (Fig. 2). CPC did not show interaction with other antibodies and proteins. CPC had selectivity to Cp149 dimer (Figure S1, S1B).

CD was measured for the core protein. DMSO treated core protein did not show significant alterations in molar ellipticity, while core protein treated with BS, a positive control, did. Also, CPC treated core protein showed a propensity for alteration, indicating that analogous conformational changes are induced in the secondary structure

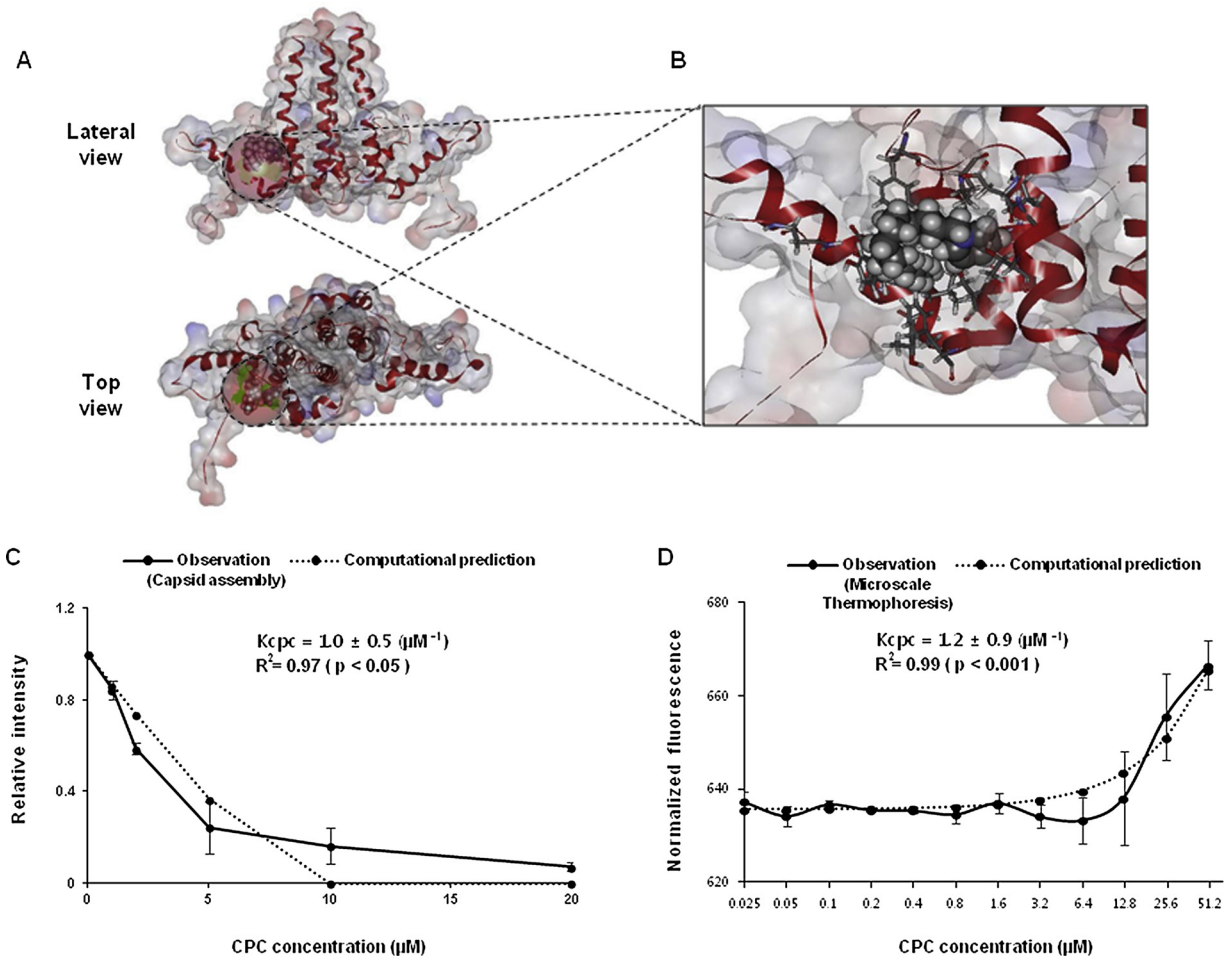

Fig. 5. Modeling and numerical interpretation of capsid assembly inhibition.
A. Cp149 dimer model and binding site candidate constructs in lateral (top) and top (bottom) view. The receptor cavity site of dimeric Cp149 for interacting with the CPC molecule is depicted as a mesh of colored dots and transparent red sphere. The CPC molecule is depicted in a CPK model.
B. Docking simulation of CPC. Residues predicted to be involved in the Cp149-CPC interaction; PHE23, PRO25, ASP29, LEU30, THR33, TRP102, SER106, PHE110, THR114, VAL115, TYR118, LEU119, and ASN136 are depicted in the stick model and CPC in the CPK model. The secondary structure of other residues in Cp149 is depicted in the flat ribbon model.
C. Capsid assembly assay with HBV Cp149 in a series of CPC concentrations. Relative capsid amount was quantified from the intensity of bands obtained by immunoblot analysis. Assembly inhibition curve and computationally extrapolated prediction curve were plotted.
D. Microscale thermophoresis assay with HBV Cp149 in a series of CPC concentrations. Normalized fluorescence intensity was interpreted by the superpositional expression of thermophoresis between capsid and dimer. Thermophoresis curve and computationally derived prediction curve were plotted.
CPC association constant, R square and P-value were noted.
Cp149, Core protein 149; CPC, Cetylpyridinium chloride; CPK, Corey-Pauling-Kortum; HBV, Hepatitis B virus.

Table 3
Inhibitor affinity derived in numerical interpretation. Capsid assembly and microscale thermophoresis results were interpreted based on the non-competitive inhibition model. Inhibitor association constants for CPC, SA, and BCM-599 were derived from arithmetic operations. R square values for the fit curve were marked separately.

Name	Capsid assembly		Microscale thermophoresis	
	association constant	R square	association constant	R square
Cetylpyridinium Chloride(CPC)	1.0 ± 0.5 (uM^{-1})	0.97	1.2 ± 0.9 (uM^{-1})	0.99
Sulfanilamide(SA)	0.11 ± 0.06 (uM^{-1})	0.96	0.3 ± 0.1 (uM^{-1})	0.99
BCM-599	0.25 ± 0.11 (uM^{-1})	0.99	0.5 ± 0.2 (uM^{-1})	0.99

(Fig. 2D).

3.3. CPC suppressed HBV biogenesis by interfering with capsid assembly

We performed sucrose density analysis using Cp149 and CPC. CPC markedly decreased the amount of capsid (Fig. 3A). Next, we determined the *in vitro* activity of CPC using HepG2.2.15 cells (Fig. 3B–D), since HepG2.2.15 cells release HBV virus particles. CPC inhibited HBV biogenesis in HepG2.2.15 cells; both intracellular and extracellular HBV DNA were significantly reduced (Fig. 3B). Meanwhile, equivalent amounts of viral RNA was measured in the control group of HepG2.2.15 cells and cells treated with CPC (Fig. 3C).

Table 4
Equations used in numerical analysis of capsid assembly inhibition. Equilibrium of CPC binding reaction (Eq. 1.) and capsid assembly reaction (Eq. 2.) were set as a competing equilibrium by sharing dimeric core protein term in both equations. Mass conservation law for core protein conservation (Eq. 3.) and CPC conservation (Eq. 4.) were formulated with concentration terms. Core association constant was derived from capsid assembly reaction equilibrium (Eq. 5.). Core protein conservation equation was recasted in terms of capsid and CPC bound dimeric core protein concentration terms using core protein association constant (Eq. 6.). CPC association constant was derived from CPC binding reaction equilibrium (Eq. 7.). CPC association constant equation was used to obtain CPC association constants. Normalized fluorescence intensity in core protein thermophoresis was formulated as a superposition of normalized fluorescence intensity terms of capsid, CPC bound core protein dimer, and unbound core protein dimer (Eq. 8.) S_T denotes soret coefficient for dimeric core protein. Soret coefficients for CPC bound and unbound dimeric core proteins are assumed to be same.

Equation number	Formula	Description
Eq. 1.	$Cp149_2 + CPC \Longleftrightarrow Cp149_2 \bullet CPC$	CPC binding equilibrium
Eq. 2.	$120Cp149_2 \Longleftrightarrow Capsid$	Capsid assembly equilibrium
Eq. 3.	$[Cp149_2]_{Total} = 120[Capsid] + [Cp149_2] + [Cp149_2 \bullet CPC]$	Core protein conservation
Eq. 4.	$[CPC]_{Total} = [Cp149_2 \bullet CPC] + [CPC]$	CPC conservation
Eq. 5.	$K_{capsid} = [Capsid]/[Cp149_2]^{120}$	Core association constant
Eq. 6.	$[Cp149_2]_{Total} = 120[Capsid] + \sqrt[120]{[Capsid]/K_{capsid}} + [Cp149_2 \bullet CPC]$	Core protein conservation recasted
Eq. 7.	$K_{CPC} = \frac{[Cp149_2 \bullet CPC]}{([CPC]_{Total} - [Cp149_2 \bullet CPC])\sqrt[120]{[Capsid]/K_{capsid}}}$	CPC association constant
Eq. 8.	$F_{norm} = \frac{25[Capsid](1 - 50S_T\Delta T) + ([Cp149_2] + [Cp149_2 \bullet CPC])(1 - S_T\Delta T)}{25[Capsid] + [Cp149_2] + [Cp149_2 \bullet CPC]}$	Thermophoresis fluorescence intensity

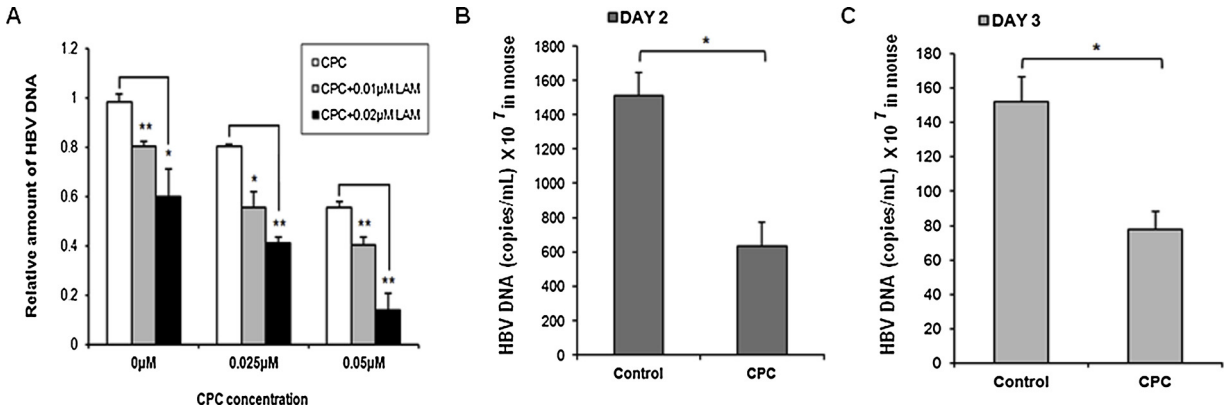

Fig. 6. Antiviral activity of CPC in a mouse model of HBV infection and combinational effect of CPC and LAM.
A. Relative virion concentrations after different combination treatments with CPC and LAM.
B-C. Mice serum HBV DNA levels after 2day (B) and 3day (C) CPC (30 μg/kg) intramuscular injection analyzed by quantitative real time-PCR. Control group was injected intramuscularly with DMSO (1:1000 dilution).
Values are mean ± standard error of the mean (SEM, n = 4 per group); $*p < 0.05$, $**p < 0.01$, *t* test.
CPC, Cetylpyridinium chloride; LAM, Lamivudine; HBV, Hepatitis B virus.

HepG2.2.15 cells showed consistent cell viability when treated with CPC concentrations between 0–1 μM (Fig. 3D).TEM images also showed that capsid assembly inhibition was induced by CPC (Fig. 4). TEM images of capsid assembly with no treatment displayed that circular particles with diameters of 30–35 nm were detected, and resembled bright rings with dark centers (Fig. 4B, C). However, CPC decreased capsid formation; capsid particles exhibited ruptures and asymmetric modifications (Fig. 4D, E, Table 2).

3.4. Docking modeling between HBV Cp149 dimer and CPC using in silico computer simulation

The single bonds of the CPC along the saturated hydrocarbon chain are rotatable (Meleshyn, 2009). Among the computed candidate binding sites, a groove-like structure located between residues 23–33, 102–119, and 136 with a volume of 96 cubic angstrom, was given multiple possible conformations for receptor-ligand docking (Venkatachalam et al., 2003) (Fig. 5A, B). The flexible carbon chain was reshaped to fit into the Cp149 dimer cavity; the interaction energy stabilized the Cp149 dimer-CPC complex. The groove structures in dimeric and hexameric Cp149, differed in spatial occupation and ligand accessibility. Surface-to-volume ratio of the cavity was larger and more partitioned in the hexameric model. In addition, hexameric Cp149 required conformational compression along the inter-dimer interaction residues. C-terminal residues, compressed by the neighboring dimer, enclosed the groove structure, which obstructed ligand access. The structure in dimeric Cp149 was found to be more relaxed and capable of ligand binding. The binding strength between Cp149 dimer and CPC was 8.5 kcal/mol. CPC was predicted to be capable of binding to dimeric CP149 (Fig. 5). The results were consistent with thermophoresis outputs in monolith assay (Fig. 2A–C), thus confirming that CPC binds directly to the HBV Cp149 dimer (Leis et al., 2010).

3.5. Numerical illustration of CPC arisen constrain on capsid assembly

In the HBV capsid structure, a dimeric core protein subunit binds to 4 adjacent dimer core protein subunits (Wynne et al., 1999). From the docking simulation model, the binding site of CPC on dimeric core protein was predicted not to be the binding sites between adjacent dimeric core protein subunits in capsid structure (Figure S2A). Virtual mole fraction coefficient of capsid was derived as 25 from symmetric capsid model (Figure S2B). Accordingly, we hypothesized that CPC is a non-competitive inhibitor and set a competing equilibrium between binding of CPC and capsid assembly (Figure S2C). Inhibitor association constants K_i for CPC, SA and BCM-599 were calculated from the capsid assembly results (Figs. 5, S3) (Cho et al., 2014). The capsid assembly

Table 5
IC_{50} values and CI index of inhibitor cetylpyridinium chloride - lamivudine cocktails. Variable combinational treatment of CPC and LAM was analyzed using the compusyn program. Combination ratio defined as CPC concentration to LAM concentration (12, 4, 3, 2, 1.5, 1, 0.67, 0.5, and 0.33: 1) were treated with LAM concentrations (0.01, 0.02, 0.05, 0.1, 0.2, 0.5, and 1 μM). HepG2.2.15 extracellular HBV DNA was collected and quantified using real time PCR. Drug inhibitory effect was calculated as the fraction of decrease in HBV viral DNA compared to the control. IC_{50} (μM) and CI-values were analyzed for individual ratios. Synergistic effect is marked from normal indication for reference.

Combination ratio	IC_{50}(μM)	CI-value	Synergic effect
Pure CPC	0.25	1	+ + +
12 : 1	0.154	0.551	
4 : 1	0.140	0.376	+ + +
3 : 1	0.145	0.796	+ +
2 : 1	0.102	0.803	+ +
1.5 : 1	0.105	0.811	+ +
1 : 1	0.079	0.875	+
0.67 : 1	0.076	0.862	+
0.5 : 1	0.078	1.110	–
0.33 : 1	0.065	0.920	±
Pure 3TC	0.023	1	

All combination ratios are expressed as (CPC amount): (Lamivudine amount) was calculated with Compusyn software.
IC_{50} is half maximal inhibitory concentration that means measure of the potency of substance in inhibiting a specific biological function.
CI-value (Combination index) is a criteria that indicates synergism, additive effect and antagonism.

inhibition was plotted with the prediction curve, which was extrapolated with the CPC association constant (Fig. 5C, Table 3). Microscale thermophoresis data was analyzed and plotted with the computed thermophoresis curve (Fig. 5D, Table 4). The CPC binding association constant was calculated to be 1.0 ± 0.5 μM^{-1} in capsid assembly, while in the monolith assay, the optimal association constant was 1.2 ± 0.9 μM^{-1} (Fig. 5C, D). SA and BCM-599 showed weaker associations compared to CPC (Figure S3, Table 3).

3.6. Combination of CPC and LAM shows synergistic effect

When treated with both CPC and LAM, HBV virion concentration decreased more compared to single treatments of CPC and LAM alone (Fig. 6A). To determine whether treatment of both CPC and LAM reduced the HBV viral concentration synergistically, we calculated CI values using a dose-effect curve (Figure S4A), a combination of index plot (Figure S4B), and an isobologram (Figure S4C) marked by CPC, LAM, and Mix (CPC + LAM). As a result, we confirmed that the virion concentration was reduced synergistically because of CPC and LAM treatment (Figs. 6A, S4). In particular, 0.142 μM CPC with 0.012 μM LAM, and 0.112 μM CPC with 0.028 μM LAM showed strong synergistic effects (Table 5).

3.7. CPC showed antiviral effect in a mouse model of HBV infection

We tested the anti-HBV activity of CPC using mouse model. CPC suppressed serum HBV DNA levels, decreased by 60% in day2 and 45% in day3 compared to the control (Fig. 6B, C). These results demonstrate that CPC represses HBV biogenesis by inhibiting the conversion of dimeric Cp149 to capsid structures through receptor ligand interaction with free dimeric subunits (Figure S4D). Together, these findings indicate that CPC is a potent drug for abolishing HBV.

4. Discussion

Nucleos(t)ide analogues such as adefovir, tenofovir, and entecavir have been used for treating patients with HBV-related liver diseases (Fabrizi et al., 2004). These drugs target RTs, however, RT-targeting drugs have low efficiency, which leads to increasingly high drug dose and drug resistance (Fabrizi et al., 2004). Therefore, new potent antiviral compounds capable of inhibiting viral proliferation through distinct mechanisms are highly desired (Dawood et al., 2017). We tested HBV capsid assembly inhibition effect for 978 FDA-approved drugs for novel drug compound selection and compared CPC with other previously known capsid assembly inhibitors (SA, BS) (Cho et al., 2013). The viral life cycle of HBV, including virion maturation and genome duplication, is highly dependent on capsid assembly (Yang and Lu, 2017). Accordingly, capsid assembly inhibition is a good antiviral target for HBV treatment to effectively suppress HBV infection (Ren et al., 2017). Thus, in this study, we focused on searching for potential drug compound that inhibits HBV capsid assembly. Among the 978 FDA-approved drug compounds (Cat.L1300, 978 drug compounds library version, Selleckchem, Houston, USA), we selected CPC as an effective candidate that reduces viral replication. CPC selectively interacted with HBV core protein dimer and inhibited capsid assembly *in vitro* (Figs. 1A, B, S1B). CPC also showed an insignificant impact on cell viability (up to 1 μM) while reducing the number of virus particles in HepG2.2.15 cells that release HBV virus and mice that possess HBV virus with hydrodynamic model system (Figs. 3B–D, 6 B, C). It can be deduced that CPC is an effective anti-HBV capsid assembly inhibitor. Nonetheless, further studies including examination on combination effect between CPC and HBV reverse transcriptase inhibitors other than lamivudine and confirmation of CPC antiviral effect in diverse *in vivo* conditions including mouse models are needed.

CPC functions as an antiseptic that kills bacteria and other organisms (Lee et al., 2017). It has also been widely used in pesticides and mouthwashes (Lee et al., 2017). According to the ADMET data, CPC had low penetration and absorption due to its hydrophobicity and low polar surface area, which are disadvantageous for drug delivery (Table 1). For use in clinical settings, a sufficient plasma concentration must be achieved. Therefore, we propose supplements that can help penetrate cells to maximize the inhibitory effect of CPC.

There are several nucleos(t)ide analogues, including LAM, that target HBV-RT (Stein and Loomba, 2009). We showed a synergistic effect on HBV replicative inhibition in HepG2.2.15 cell when treated with both LAM and the capsid assembly inhibitor CPC (Fig. 6A). Similarly, our previous study reported that the capsid assembly inhibitor BCM-599 also showed a synergistic effect when treated with LAM (Cho et al., 2014). Intracellular replication is expected to increase by capsid assembly increase. Also it is reported that HBV capsid assembly is believed to activate the reverse transcription (Ceres et al., 2004). Thus, it is conceivable that reverse transcription stage, of which nucleoside analogues target, and capsid assembly stage, of which CPC targets, may not be independent and give rise to the synergistic effect. Inhibition of the encapsidation stage may reduce the amount of pgRNA encapsidated within the viral capsid and subsequently influence the reverse transcriptase inhibition. Synergistic effect may be expressed through such mechanism. Together, these results indicated effective HBV viral biogenesis inhibition induced by co-treatment with nucleos(t)ide analogue drugs and capsid assembly inhibitors.

Here, we identified CPC as a novel HBV inhibitor with *in vivo* and *in vitro* systems and demonstrated that CPC induces HBV inhibition through inhibition of viral capsid assembly. These effects were confirmed by TEM and mouse model. Overall, our findings contribute to the development of effective inhibitors against HBV biogenesis.

Conflict of interest

None declared.

Acknowledgements

This work was supported by a grant of the Korea Health Technology

R&D Project through the Korea Health Industry Development Institute (KHIDI), funded by the Ministry of Health & Welfare. Republic of Korea [HI16C1074] and the Seoul National University Hospital Research Fund [0420160300 (2016-1073)].

Appendix A. Supplementary data

Supplementary material related to this article can be found, in the online version, at doi:https://doi.org/10.1016/j.virusres.2019.01.004.

References

Baaske, P., Wienken, C.J., Reineck, P., Duhr, S., Braun, D., 2010. Optical thermophoresis for quantifying the buffer dependence of aptamer binding. Angew. Chem. Int. Ed. Engl. 49 (12), 2238–2241.

Brunetto, M.R., Lok, A.S., 2010. New approaches to optimize treatment responses in chronic hepatitis B. Antivir. Ther. (Lond.) 15 (Suppl 3), 61–68.

Ceres, P., Stray, S.J., Zlotnick, A., 2004. Hepatitis B virus capsid assembly is enhanced by naturally occurring mutation F97L. J. Virol. 78 (17), 9538–9543.

Cho, M.H., Song, J.S., Kim, H.J., Park, S.G., Jung, G., 2013. Structure-based design and biochemical evaluation of sulfanilamide derivatives as hepatitis B virus capsid assembly inhibitors. J. Enzyme Inhib. Med. Chem. 28 (5), 916–925.

Cho, M.H., Jeong, H., Kim, Y.S., Kim, J.W., Jung, G., 2014. 2-amino-N-(2,6-dichloropyridin-3-yl)acetamide derivatives as a novel class of HBV capsid assembly inhibitor. J. Viral Hepat. 21 (12), 843–852.

Choi, Y., Gyoo Park, S., Yoo, J.H., Jung, G., 2005. Calcium ions affect the hepatitis B virus core assembly. Virology 332 (1), 454–463.

Chou, T.C., 2006. Theoretical basis, experimental design, and computerized simulation of synergism and antagonism in drug combination studies. Pharmacol. Rev. 58 (3), 621–681.

Chou, T.C., 2010. Drug combination studies and their synergy quantification using the chou-talalay method. Cancer Res. 70 (2), 440–446.

Dawood, A., Abdul Basit, S., Jayaraj, M., Gish, R.G., 2017. Drugs in development for hepatitis B. Drugs 77 (12), 1263–1280.

Doong, S.L., Tsai, C.H., Schinazi, R.F., Liotta, D.C., Cheng, Y.C., 1991. Inhibition of the replication of hepatitis B virus in vitro by 2',3'-dideoxy-3'-thiacytidine and related analogues. Proc. Natl. Acad. Sci. U. S. A. 88 (19), 8495–8499.

Fabrizi, F., Dulai, G., Dixit, V., Bunnapradist, S., Martin, P., 2004. Lamivudine for the treatment of hepatitis B virus-related liver disease after renal transplantation: meta-analysis of clinical trials. Transplantation 77 (6), 859–864.

Garson, J.A., Grant, P.R., Ayliffe, U., Ferns, R.B., Tedder, R.S., 2005. Real-time PCR quantitation of hepatitis B virus DNA using automated sample preparation and murine cytomegalovirus internal control. J. Virol. Methods 126 (1-2), 207–213.

Hirsch, R.C., Lavine, J.E., Chang, L.J., Varmus, H.E., Ganem, D., 1990. Polymerase gene products of hepatitis B viruses are required for genomic RNA packaging as wel as for reverse transcription. Nature 344 (6266), 552–555.

Kang, H.Y., Lee, S., Park, S.G., Yu, J., Kim, Y., Jung, G., 2006. Phosphorylation of hepatitis B virus Cp at Ser87 facilitates core assembly. Biochem. J. 398 (2), 311–317.

Kim, Y.S., Seo, H.W., Jung, G., 2015. Reactive oxygen species promote heat shock protein 90-mediated HBV capsid assembly. Biochem. Biophys. Res. Commun. 457 (3), 328–333.

Lee, M.J., Song, H.J., Jeong, J.Y., Park, S.Y., Sohn, U.D., 2013. Anti-oxidative and anti-inflammatory effects of QGC in cultured feline esophageal epithelial cells. Korean J. Physiol. Pharmacol. 17 (1), 81–87.

Lee, J.E., Lee, J.M., Lee, Y., Park, J.W., Suh, J.Y., Um, H.S., Kim, Y.G., 2017. The antiplaque and bleeding control effects of a cetylpyridinium chloride and tranexamic acid mouth rinse in patients with gingivitis. J. Periodontal Implant Sci. 47 (3), 134–142.

Leis, S., Schneider, S., Zacharias, M., 2010. In silico prediction of binding sites on proteins. Curr. Med. Chem. 17 (15), 1550–1562.

Lott, L., Beames, B., Notvall, L., Lanford, R.E., 2000. Interaction between hepatitis B virus core protein and reverse transcriptase. J. Virol. 74 (24), 11479–11489.

Meleshyn, A., 2009. Cetylpyridinium chloride at the mica-water interface: incomplete monolayer and bilayer structures. Langmuir 25 (2), 881–890.

Ott, J.J., Stevens, G.A., Groeger, J., Wiersma, S.T., 2012. Global epidemiology of hepatitis B virus infection: new estimates of age-specific HBsAg seroprevalence and endemicity. Vaccine 30 (12), 2212–2219.

Pan, H.Y., Pan, H.Y., Song, W.Y., Zheng, W., Tong, Y.X., Yang, D.H., Dai, Y.N., Chen, M.J., Wang, M.S., Huang, Y.C., Zhang, J.J., Huang, H.J., 2017. Long-term outcome of telbivudine versus entecavir in treating higher viral load chronic hepatitis B patients without cirrhosis. J. Viral Hepat. 24 (Suppl. 1), 29–35.

Paradis, V., 2013. Histopathology of hepatocellular carcinoma. Recent Results Cancer Res. 190, 21–32.

Popkin, D.L., Zilka, S., Dimaano, M., Fujioka, H., Rackley, C., Salata, R., Griffith, A., Mukherjee, P.K., Ghannoum, M.A., Esper, F., 2017. Cetylpyridinium chloride (CPC) exhibits potent, rapid activity against influenza viruses in vitro and in vivo. Pathog. Immun. 2 (2), 252–269.

Rao, S.N., Head, M.S., Kulkarni, A., LaLonde, J.M., 2007. Validation studies of the site-directed docking program LibDock. J. Chem. Inf. Model. 47 (6), 2159–2171.

Ren, Q., Liu, X., Luo, Z., Li, J., Wang, C., Goldmann, S., Zhang, J., Zhang, Y., 2017. Discovery of hepatitis B virus capsid assembly inhibitors leading to a hetero-aryldihydropyrimidine based clinical candidate (GLS4). Bioorg. Med. Chem. 25 (3), 1042–1056.

Seeger, C., Mason, W.S., 2000. Hepatitis B virus biology. Microbiol. Mol. Biol. Rev. 64 (1), 51–68.

Shim, H.Y., Quan, X., Yi, Y.S., Jung, G., 2011. Heat shock protein 90 facilitates formation of the HBV capsid via interacting with the HBV core protein dimers. Virology 410 (1), 161–169.

Smith, J.R., Evans, K.J., Wright, A., Willows, R.D., Jamie, J.F., Griffith, R., 2012. Novel indoleamine 2,3-dioxygenase-1 inhibitors from a multistep in silico screen. Bioorg. Med. Chem. 20 (3), 1354–1363.

Stein, L.L., Loomba, R., 2009. Drug targets in hepatitis B virus infection. Infect. Disord. Drug Targets 9 (2), 105–116.

Timofeeva, O.A., Chasovskikh, S., Lonskaya, I., Tarasova, N.I., Khavrutskii, L., Tarasov, S.G., Zhang, X., Korostyshevskiy, V.R., Cheema, A., Zhang, L., Dakshanamurthy, S., Brown, M.L., Dritschilo, A., 2012. Mechanisms of unphosphorylated STAT3 transcription factor binding to DNA. J. Biol. Chem. 287 (17), 14192–14200.

Vanlandschoot, P., Cao, T., Leroux-Roels, G., 2003. The nucleocapsid of the hepatitis B virus: a remarkable immunogenic structure. Antiviral Res. 60 (2), 67–74.

Venkatachalam, C.M., Jiang, X., Oldfield, T., Waldman, M., 2003. LigandFit: a novel method for the shape-directed rapid docking of ligands to protein active sites. J. Mol. Graph. Model. 21 (4), 289–307.

Wu, G., Robertson, D.H., Brooks 3rd, C.L., Vieth, M., 2003. Detailed analysis of grid-based molecular docking: a case study of CDOCKER-A CHARMm-based MD docking algorithm. J. Comput. Chem. 24 (13), 1549–1562.

Wynne, S.A., Crowther, R.A., Leslie, A.G., 1999. The crystal structure of the human hepatitis B virus capsid. Mol. Cell 3 (6), 771–780.

Yang, L., Lu, M., 2017. Small molecule inhibitors of hepatitis B virus nucleocapsid assembly: a new approach to treat chronic HBV infection. Curr. Med. Chem.

Zlotnick, A., Ceres, P., Singh, S., Johnson, J.M., 2002. A small molecule inhibits and misdirects assembly of hepatitis B virus capsids. J. Virol. 76 (10), 4848–4854.

Zuckerman, A.J., 1999. More than third of world's population has been infected with hepatitis B virus. BMJ 318 (7192), 1213.